EPJ Web of Conferences **271**, 01006 (2022) https://doi.org/10.1051/epjconf/202227101006
HYP2022

Commissioning of the hypertriton binding energy measurement at MAMI

Philipp Eckert[1,*], *Patrick* Achenbach[1,**], *Takeru* Akiyama[2], *Jinhui* Chen[4,5], *Michael O.* Distler[1], *Anselm* Esser[1], *Julian* Geratz[1], *Christian* Helmel[1], *Michael* Hoek[1], *Kosuke* Itabashi[2], *Masashi* Kaneta[2], *Ryoko* Kino[2], *Pascal* Klag[1], *Yu-Gang* Ma[4,5], *Harald* Merkel[1], *Masaya* Mizuno[2], *Ulrich* Müller[1], *Sho* Nagao[2], *Satoshi N.* Nakamura[6,2], *Yuki R.* Nakamura[2], *Kazuki* Okuyama[2], *Josef* Pochodzalla[1,3], *Björn Sören* Schlimme[1], *Concettina* Sfienti[1], *Tianhao* Shao[1,4], *Marcell* Steinen[3], *Koga* Tachibana[2], *Michaela* Thiel[1], *Yuichi* Toyama[2], and *Keita* Uehara[2] for the A1 Collaboration

[1]Institute for Nuclear Physics, Johannes Gutenberg University Mainz, 55099 Mainz, Germany
[2]Graduate School of Science, Tohoku University, Sendai, Miyagi 980-8578, Japan
[3]Helmholtz Institute Mainz, GSI Helmholtzzentrum für Schwerionenforschung, Darmstadt, Johannes Gutenberg University Mainz, 55099 Mainz, Germany
[4]Key Laboratory of Nuclear Physics and Ion-beam Application (MOE), Institute of Modern Physics, Fudan University, Shanghai 200433, China
[5]Shanghai Research Center for Theoretical Nuclear Physics, NSFC and Fudan University, Shanghai 200438, China
[6]Department of Physics, Graduate School of Science, The University of Tokyo, Tokyo 113-0033, Japan

Abstract. A high-precision hypernuclear experiment has been commissioned at the Mainz Microtron (MAMI) to determine the hypertriton Λ binding energy via decay-pion spectroscopy. The method has been successfully pioneered with ${}^{4}_{\Lambda}$H studies in the last decade. The experiment makes use of a novel high luminosity lithium target with a length of 45 mm while being only 0.75 mm thick to keep momentum smearing of the decay pions low. The target-to-beam alignment as well as the observation of the deposited heat is achieved with a newly developed thermal imaging system. Together with a precise beam energy determination via the undulator light interference method a recalibration of the magnetic spectrometers will be done to obtain a statistical and systematic error of about 20 keV. The experiment started in the summer of 2022 and initial optimization studies for luminosity and data quality are presented.

1 Λ binding energies of hydrogen hypernuclei

The hypertriton, ${}^{3}_{\Lambda}$H, is the simplest known hypernucleus and therefore a benchmark nucleus for hypernuclear structure calculations. It plays a fundamental role in strangeness nuclear physics, comparable to the deuteron in non-strange nuclear physics. Its Λ binding energy is of high importance for understanding the Λ–N interaction and can be used to constrain state-of-the-art calculations which describe the internal structure of ${}^{3}_{\Lambda}$H .

*e-mail: eckert@uni-mainz.de
**Now at Thomas Jefferson National Accelerator Facility (JLab), Newport News, Virginia 23606, USA

For almost 50 years, the most precise binding energy value is given by $B_\Lambda = 130 \pm 50\,\text{keV}$, averaged and compiled by Jurič et al. from emulsion experiments [1, 2]. Just recently, two new values became available, one by the STAR Collaboration [3], $B_\Lambda = 406 \pm 120\,(\text{stat.}) \pm 110\,(\text{syst.})\,\text{keV}$, and one by the ALICE Collaboration [4], $B_\Lambda = 72 \pm 63\,(\text{stat.}) \pm 36\,(\text{syst.})\,\text{keV}$.

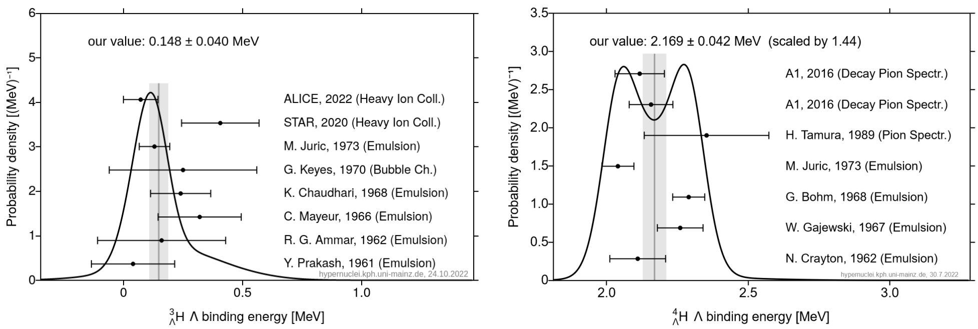

Figure 1. Ideograms of the world data sets on Λ binding energy measurements for ${}^{3}_{\Lambda}\text{H}$ (left) and ${}^{4}_{\Lambda}\text{H}$ (right) [5]. The error bars include statistical and systematic uncertainties. In case of ${}^{4}_{\Lambda}\text{H}$, the data have been conservatively handled by computing a scaling factor $S = \sqrt{\chi^2/ndf}$ and multiplying it with the error. Our averages are $B_\Lambda({}^{3}_{\Lambda}\text{H}) = 0.148 \pm 0.040\,\text{MeV}$ and $B_\Lambda({}^{4}_{\Lambda}\text{H}) = 2.169 \pm 0.042\,\text{MeV}$.

Remarkably, the STAR value is about 8 times larger than the preliminary one from ALICE and they differ by two standard deviations. The STAR value also seems to be in tension with the emulsion value. This data situation along with other earlier measurements is visualized in an ideogram in the left panel of Fig. 1, obtained from the Chart of Hypernuclides [5]. An average value of $\overline{B_\Lambda} = 148 \pm 40\,\text{keV}$ is computed with a relative error of still more than 25 %. It is to be noted, that in many cases the emulsion data values are missing a systematic error. So for these values, a systematic error of $\pm\,40\,\text{keV}$, given in Davis' reviews [6, 7], has been included in these averages. This is the so-far best estimate for the accuracy of these emulsion values.

In the right panel of Fig. 1 the ideogram for ${}^{4}_{\Lambda}\text{H}$ is shown, including two values from previous decay-pion experiments by the A1 Collaboration [8, 9] and several emulsion values [1, 2]. Correlated errors in the A1 data were treated explicitly adopting the PDG procedure [10]. The resulting probability density distribution has a structure with two maxima and a $\chi^2/ndf = 12.5/6$ greater than 1, but still with a p value of 0.05, suggesting that the errors of one or more contributing measurements are underestimated. Not knowing which of the errors are underestimated, for averaging they are all multiplied by the same factor $\sqrt{\chi^2/ndf}$, again analogous to the PDG [11]. The resulting relative error of the average is ∼ 20 %.

As the data situation for these light hypernuclei is clearly not satisfactory, a new high-precision experiment via decay-pion spectroscopy has been commissioned at MAMI with the goal to reach a 20 keV total error in the binding energy [12, 13]. Within the running experiment, both, ${}^{3}_{\Lambda}\text{H}$ and ${}^{4}_{\Lambda}\text{H}$, are expected to be observed.

2 Decay-pion spectroscopy at MAMI

2.1 Experimental technique

In general, hypernuclei can be produced from a target nucleus with a high-energy electron beam. The underlying process is the strangeness electroproduction, converting a proton to a

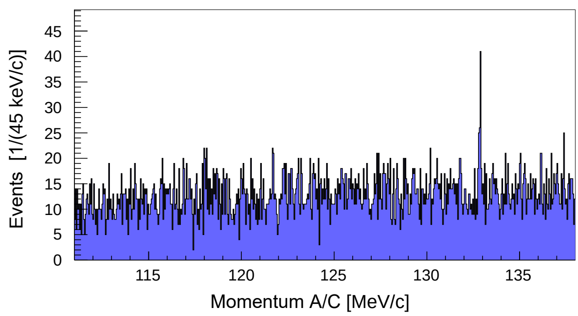

Figure 2. Momentum spectrum for strangeness tagged pions from the 2014 measurement at MAMI [14]. Mono-energetic decay-pions of ${}^{4}_{\Lambda}$H were observed at ~ 133 MeV/c. A signal from two-body decays of stopped ${}^{3}_{\Lambda}$H was not found at the expected momentum of ~ 114 MeV/c.

$\Lambda - K^{+}$ pair. If this Λ stays bound to the nucleus, a highly excited hypernucleus is formed. This will eventually de-excitate, possibly by the emission of one or more other nucleons, so that finally a smaller hypernuclear isotope in its ground state remains. Due to the comparably long Λ lifetime of $\tau_{\Lambda} = 263$ ps, the hypernucleus is expected to survive the production process as well as the loss of recoil momentum inside the target material, giving the opportunity to observe the decay of the hypernucleus at rest. In this experiment we are looking for the charged pionic two-body decay, which is mono-energetic. Hence, the mass of the hypernucleus $m_{\text{hyp}} = \sqrt{m_{\text{nucl}}^2 + p_{\pi}^2} + \sqrt{m_{\pi}^2 + p_{\pi}^2}$ can be determined by measuring the momentum of the decay-pions p_{π} with the magnetic spectrometers. The pion and nucleus masses are precisely known.

The probability for the formation of a hypernucleus is low compared to background events generated by other processes. In the experiment the KAOS spectrometer is used to detect the kaons in coincidence with the decay pions in the two spectrometers A and C. In that way "strangeness tagged" events can be identified. This method was successfully used at MAMI within the last decade [8, 14]. In that time, beryllium targets of thicknesses between 23 and 47 mg/cm^2 were used. Fig. 2 shows a representative momentum spectrum, where decay pions of ${}^{4}_{\Lambda}$H are clearly visible at around 133 MeV/c, resulting in a binding energy of $B_{\Lambda} = 2.157 \pm 0.005\,(\text{stat.}) \pm 0.077\,(\text{syst.})$ MeV. The systematic error was strongly dominating because the spectrometer calibration was limited by the available MAMI beam energy measurement with an accuracy of 160 keV. However, the beam spread and instability are known to be much smaller. Consequently, an improved beam energy measurement can reduce the error of the experiment. This will be made possible by the novel undulator light interference method with an accuracy of 18 keV [15].

2.2 Novel high-luminosity lithium target

Lithium is expected to have a higher ${}^{3}_{\Lambda}$H yield compared to beryllium, since it offers fewer fragmentation possibilities into other hypernuclei. Also, due to its low density of 0.534 g/cm^3, it allows for a completely new target geometry, shown in Fig. 3. Here, a length of 45 mm lithium will be traversed by the electron beam resulting in a total thickness of 2.5 g/cm^2. This is around 100 times thicker than the previous target to maximize the production rate of hypernuclei while minimizing the accidental background by radiation contamination, since the beam current can be reduced. At the same time, the lithium sheet

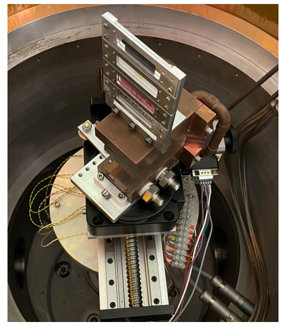

Figure 3. High-luminosity lithium target used for the hypertriton experiment. Left: The lithium sheet has a thickness of 2.5 g/cm^2 in beam direction. In the left part of the setup, pipes for the cooling liquid can be seen for the optimal removal of heat from the lithium sheet. Parts of the copper frame are painted with infrared absorbing black paint to prevent undesired reflections in the camera pictures. Right: The copper frame mounted inside the target chamber, additional targets on top. Below the frame, a rotary and a linear stepper motor are located.

is 750 μm thin perpendicular to the beam direction to minimize the amount of material to be traversed by the exiting decay pions.

Metallic lithium is challenging to handle due to its low melting point of 180°C and its high reactivity even with ambient air. To keep it below melting temperature during the experiment, it is mounted inside a water-cooled copper frame. Regarding the reactivity, lithium can be handled inside an argon atmosphere. However, the spatial alignment of the target inside the target chamber cannot be done with the common theodolite techniques, since the contact time with air would be too long. Therefore, the target holder is mounted onto a rotary and a linear motor to move the target into the correct position during the experiment. To observe the temperature of the lithium while being warmed up by the electron beam, a thermal camera surveillance was installed onto the target chamber. This serves the two purposes of measuring the target temperature as well as extracting information about the alignment from the heat distribution. Examples of this can be seen in Fig. 4. On the left, the target is rotated against the electron beam, so that it is only partially warmed up. On the right side, the full amount of lithium is traversed by the electrons. These pictures were taken with a beam intensity of 2 μA and the resulting temperature was around 28°C, equivalent to 23°C above the cooling water temperature.

Also the spectrometer rates give a good indication on how the target is aligned. In another study the linear as well as the rotary position of the target was varied with the step motors and the resulting rates were observed. By that, also the ideal target position can be found, see Fig. 5. In both cases, a clear peak can be seen.

3 Hypertriton experiment commissioning in 2022

With the commissioning of the complete spectrometer setup consisting of KAOS and the A1 spectrometers A and C, roughly 100 h decay pion spectroscopy data could already be taken. The used beam energy and current are 1508 MeV/c and 500 nA, respectively. The data taking rate was at around 60 Hz. Initially it was planned to use larger beam currents of up to 5 μA, but it was observed that this exceeds the maximum particle rate KAOS is capable of. One reason is that at around 1.6 μA the KAOS trigger reaches a maximal rate of 620 kHz, seen on the left panel of Fig. 6. For higher currents the rate even dropped due to overflow issues. The other

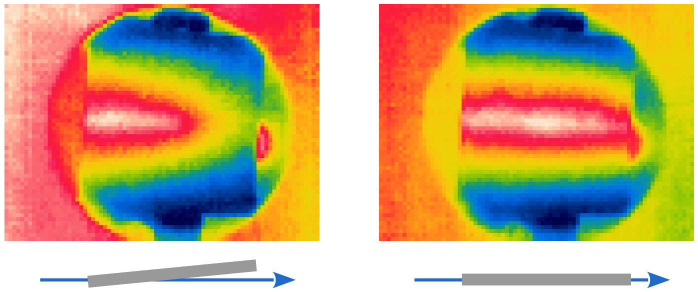

Figure 4. Thermal images of the lithium target during recent tests with a 1.5 GeV electron beam at MAMI. The orientation of the target with respect to the beam is schematically depicted at the bottom. Left: Target and beam misaligned, the lithium was only partially heated. Right: Correct alignment, the heat is equally distributed. In both cases a beam intensity of 2 μA was used and the maximum temperature of 28°C hardly exceeded room temperature. The red spot on the right side of the target results from a flange of the vacuum system in the background.

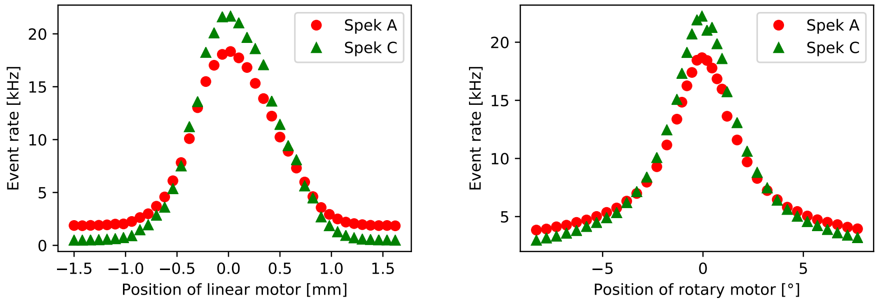

Figure 5. Spectrometer rates in relation to the target position. Left: the linear position of the target parallel to the beam was changed. Right: the rotary position was changed. In both cases, 855 MeV electrons with 3 μA beam current were used.

even more limiting reason is the quality of the recorded KAOS data, which decreases due to growing ambiguities in the reconstruction of multiple particle tracks inside the spectrometer. A measure for this is the amount of reconstructed true $\pi^+ - \pi^-$ coincidences per time between KAOS and either spectrometer A or C. As one can see in the right panel of Fig. 6, this rate initially increased linearly for low beam currents, but reached a maximum at around 600 nA. After that, the rate dropped rapidly, until at 1000 nA almost no coincidence events were reconstructed anymore. While 600 nA seemed to offer the highest rate compared to other currents, 500 nA yielded a 50% better signal to noise ratio. Therefore, it was decided to use 500 nA for the first data taking period.

Facing the second data taking period in September 2022, adjustments at the lead absorber inside KAOS will be made. Its purpose is to suppress the huge background by positrons, while still enabling kaons to enter the scintillators [16]. Right now, it is varying in thickness, being 100 mm for the low momentum range and 120 mm for the high range. Since especially at low momenta the event rate turned out to be the highest, the absorber thickness will be evened out to be 120 mm everywhere. By that, KAOS will be able to handle higher beam currents.

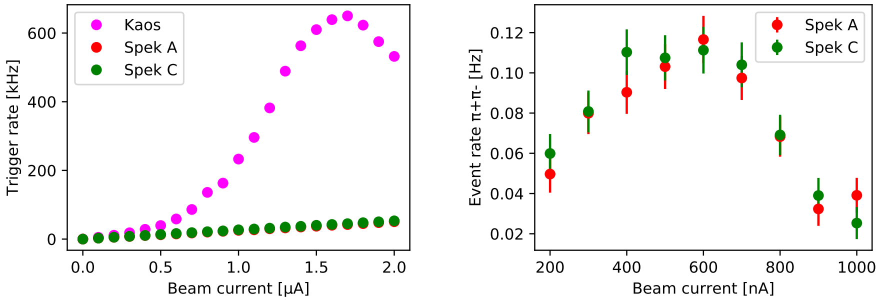

Figure 6. Rate study with the three spectrometers. Left: Trigger rate of the three spectrometers. While A and C are comparably low and continuously rising with the beam current, KAOS sees far more particles leading to a saturation of the trigger logic at around 1.6 μA before the rates drop even lower. Right: Rate of true particle coincidences of KAOS with A or C. Here, after a linear increase, a maximum at 600 nA can be seen. This is due to growing track reconstruction ambiguities with higher particle multiplicities in KAOS.

Acknowledgements

This project is supported by the Deutsche Forschungsgemeinschaft, Grant Number PO256/7−1 and the European Union's Horizon 2020 research and innovation programme No. 824093. The work is partially supported by JSPS KAKENHI Grant Numbers JP18H05459, 18H01219, 17H01121, 120002001, 15684005, 16GS0201 and GP-PU, Tohoku University. The presented data were in part collected within the framework of the PhD thesis of Philipp Eckert at the Johannes Gutenberg University Mainz.

References

[1] M. Jurić et al., Nucl. Phys. B **52**, 1 (1973)
[2] G. Bohm et al., Nucl. Phys. B **4**, 511 (1968)
[3] J. Adam et al. (STAR), Nat. Phys. **16**, 409 (2020)
[4] ALICE (2022), `2209.07360`
[5] P. Eckert, P. Achenbach et al., *Chart of hypernuclides — Hypernuclear structure and decay data* (2021), hypernuclei.kph.uni-mainz.de
[6] D.H. Davis, Nucl. Phys. A **547**, 369 (1992)
[7] D.H. Davis, Nucl. Phys. A **754**, 3c (2005)
[8] A. Esser et al. (A1), Phys. Rev. Lett. **114**, 232501 (2015)
[9] F. Schulz et al. (A1), Nucl. Phys. A **954**, 149 (2016)
[10] Particle Data Group, Prog. Theor. Exp. Phys. **2020**, 083C01 (2020)
[11] C.G. Wohl et al. (Particle Data Group), Rev. Mod. Phys. **56**, S1 (1984)
[12] P. Achenbach, S. Bleser, J. Pochodzalla, M. Steinen, PoS (Hadron2017) **207**, 1 (2018)
[13] P. Eckert, P. Achenbach, M. Aragonès Fontboté, T. Akiyama, M.O. Distler, A. Esser, J. Geratz, M. Hoek, K. Itabashi, M. Kaneta et al., PoS **PANIC2021**, 201 (2022)
[14] F. Schulz, Ph.D. thesis, Johannes Gutenberg-Universität, Mainz (2016)
[15] P. Klag et al., Nucl. Instrum. Methods Phys. Res. A **910**, 147 (2018)
[16] A. Esser, Ph.D. thesis, Johannes Gutenberg-Universität, Mainz (2013)